Phase field simulation on microstructure evolution in solidification and aging process of squeeze cast magnesium alloy

2015 IOP Conf. Ser.: Mater. Sci. Eng. 84 012065

(http://iopscience.iop.org/1757-899X/84/1/012065)

Phase field simulation on microstructure evolution in solidification and aging process of squeeze cast magnesium alloy

H W Pan [1], G M Han [1], Z Q Han [1,3] and B C Liu [1,2]

[1]Key Laboratory for Advanced Materials Processing Technology (Ministry of Education), School of Materials Science and Engineering, Tsinghua University, Beijing 100084, China
[2]State Key Laboratory of Automotive Safety and Energy, Department of Automotive Engineering, Tsinghua University, Beijing 100084, China

E-mail: zqhan@tsinghua.edu.cn

Abstract. Phase-field models have been developed to simulate the dendritic growth in pressurized solidification of Mg-Al alloy during squeeze casting and the precipitation of multi-variant β-$Mg_{17}Al_{12}$ phases during the subsequent aging process. For the pressurized solidification, the effects of pressure on the Gibbs free energy and chemical potential of solid and liquid phases, and the solute diffusion coefficient were considered. For the precipitation during aging process, the effects of elastic strain energy, anisotropy of interfacial energy, and anisotropy of interface mobility coefficient were considered. The results showed that the dendritic growth rate tends to increase and the secondary dendrite arms are more developed as the pressure is increased from 0.1 to 100MPa, which showed a good agreement with the experimental results of direct squeeze casting of Mg-Al alloy. The 2D and 3D simulated precipitates had lath shapes with lozenge ends, and the precipitate variants were parallel to the basal plane and oriented in directions with an angular interval of 60 degrees, which is in good agreement with experimental observations.

1. Introduction

Magnesium alloys are important lightweight structural materials and have received increasing attention from electronic, automobile and aerospace industries [1]. Mg-Al series alloys are commonly used because of their good castability and high specific strength. Squeeze casting is an advanced near net shape materials processing technology, in which the casting solidifies under pressure, which causes plastic deformation compensating the internal volume shrinkage [2]. Moreover, the squeeze cast products can be heat treated to further improve the mechanical properties. According to the Mg-Al binary phase diagram, eutectic β phase dissolves during solid solution, and precipitate forms during aging process, which is an important strengthening in Mg-Al based alloys [3]. Due to the advantages of high casting integrity and excellent mechanical properties of products, squeeze casting of Mg-Al alloy gains importance in the lightweighting of automobiles. To understand the solidification mechanism

[3] Correspondent: Zhiqiang Han, Ph.D, Associate professor, School of Materials Science and Engineering, Tsinghua University, Haidian District, Beijing 100084, China.

under pressure and the precipitation process during aging of Mg-Al alloy is of great significance to the design and optimization of squeeze casting and heat treatment process of Mg-Al alloy.

Microstructure evolution in pressurized solidification has been studied experimentally for years. Under superhigh pressure of several GPa, the phase diagrams of alloys are changed significantly [4]. The pressure increases the nucleation density and decreases the solute diffusion coefficient, resulting in fine microstructure [5] and high solid solubility [6]. In squeeze casting, the effect of pressure on heat transfer between the casting and the mold has been studied based on the solidification cooling curves [7, 8]. The enhanced heat transfer due to the applied pressure increases the cooling rate, which reduces the grain size according to Yong et al. [9] and El-khair [10]. Several experimental studies have been performed to gain comprehensive understanding of the morphology and structure of the β phase, and the orientation relationship with the hexagonal close packed (hcp) matrix [11, 12]. The β phase is a stoichiometric intermetallic compound with a composition of $Mg_{17}Al_{12}$ and an α-Mn-type cubic unit cell structure. Results indicate that the precipitate has a lath-shaped morphology, with the majority of precipitates forming with the habit plane parallel to the basal planes (0001) of the matrix [13].

Phase field simulation based on solute diffusion, thermodynamic driving force and ordering potential is considered to be a powerful tool for modeling the dendritic growth during solidification and the morphology evolution of the precipitates during aging. Böttger et al. [14, 15] conducted simulation of equiaxed solidification of Mg-Al alloy based on phase field method. Börzsönyi et al. [16, 17] investigated the effects of time-periodic external forcing on dendritic solidification of CCH3, a kind of liquid crystal, by experiments and phase field modeling, and found that the oscillating pressure and heating can tune the frequency of dendritic side-branching, indicating that thermal and mechanical effects are two dominant factors in interface stability. Li et al. [18] made an early attempt to simulate the precipitates in AZ91 alloy. Later Gao et al. [19] simulated the precipitation of β1 phase in Mg–Y–Nd alloy using a phase field model and discussed the effect of elastic strain energy on the precipitation. Han et al. [20] simulated the precipitation of β-$Mg_{17}Al_{12}$ using a phase field model that considered interfacial anisotropy, and discussed the effects of the two types of solution approximation on the morphology evolution of the precipitate.

The aim of the present work is to use the phase field method to investigate the dendritic growth in pressurized solidification and the growth kinetics of β-$Mg_{17}Al_{12}$ precipitates during aging Mg-Al alloys. Phase field models coupled with thermodynamic calculation for describing the dendritic growth of Mg-Al alloy during squeeze casting and precipitation process are developed, and the simulation results are compared with experimental observations.

2. Model description

2.1. Phase filed model for pressurized solidification

A phase field model based on KKS model [21] is adopted in this work to investigate the pressurized solidification. The total free energy of the system $F(c, \eta, T)$ including chemical free energy and interfacial energy are defined as:

$$F(c,\eta,T) = \int_v \left[f(c,\eta,T) + \frac{\varepsilon^2(\varphi)}{2}(\nabla\eta)^2 \right] dv \quad (1)$$

where F is the total free energy, f is the free energy density of the system, T is absolute temperature, $\varepsilon(\varphi)$ is the gradient energy coefficient related to anisotropic interfacial energy, and φ is an angle used to describe the interfacial anisotropy. The order parameter η is defined as 1 in the bulk solid and 0 in the bulk liquid.

The chemical free energy density of the system is defined as:

$$f(c,\eta,T) = h(\eta) f^{\beta}(c_{\beta},T) + \big(1 - h(\eta)\big) f^{\alpha}(c_{\alpha},T) + w g(\eta) \quad (2)$$

where c_α and c_β are the molar fractions of Al atoms in the liquid and solid phases, respectively. $f^{\alpha}(c_{\alpha},T)$ and $f^{\beta}(c_{\beta},T)$ are the chemical free energy density of the liquid and solid phases, respectively. $g(\eta)$ is a double-well potential, and w is the height of the double-well potential. $h(\eta)$ is a monotonous function from 0 to 1. In the present work, $g(\eta)$ and $h(\eta)$ are chosen as:

$$h(\eta) = \eta^3(6\eta^2 - 15\eta + 10) \tag{3}$$
$$g(\eta) = \eta^2(1-\eta)^2 \tag{4}$$

The governing equations of phase field and concentration field are given as follows,

$$\frac{\partial \eta}{\partial t} = M(\varphi)\left(\varepsilon^2(\varphi)\nabla^2\eta - f_\eta\right) \tag{5}$$
$$\frac{\partial c}{\partial t} = \nabla\cdot(D(\eta,T)\nabla c) + \nabla\cdot\left(D(\eta,T)h'(\eta)\left(c_\alpha - c_\beta\right)\nabla\eta\right) \tag{6}$$

In the ideal solution approximation, the free energy of a phase depends on the composition and temperature under atmospheric pressure [22]. For the two phases in the Mg-Al system, the general formulas are given as:

$$G_{\mathrm{m}}^{\tau} = c_{\mathrm{Al}}G_{\mathrm{Al}}^{\tau} + (1-c_{\mathrm{Al}})\,G_{\mathrm{Mg}}^{\tau} + RT(c_{\mathrm{Al}}lnc_{\mathrm{Al}} + (1-c_{\mathrm{Al}})\,ln(1-c_{\mathrm{Al}})\,) \tag{7}$$

where G_{Al}^{τ} and G_{Mg}^{τ} are the Gibbs free energy of pure Al and Mg in the phase of τ, respectively. c_{Al} is the molar fractions of Al and R is the gas constant.

The Gibbs free energy under pressure is calculated based on the quasi-harmonic approximation and equation of state (EOS) [23] shown as follows, in which P_0 is the reference pressure.

$$G(T,P) = G(T,P_0) + \int_{P_0}^{P} V(T,P')dP' \tag{8}$$

The solute diffusion coefficient is also impacted by pressure, as the viscosity of the melt increases with the increase of pressure. The solute diffusion coefficient under pressure can be calculated as follows [24], which means that the solute diffusion coefficient decreases exponentially with the increase in pressure.

$$D^P = D_0\exp\,(-PV_0/RT) \tag{9}$$

2.2. Phase field model for precipitation

The TEM observation [13] showed that the precipitate has 12 variants. Due to the symmetric distribution of the variants in the basal plane, it is adequate to investigate the evolution of three typical precipitate variants (variant-1, variant-2 and variant-3) with an interval of 60 degrees in the simulation, thus three non-conserved quantities (the structural order parameter η_q, q=1-3) and one conserved quantity, molar fraction of the solute Al, are introduced and a phase field model for precipitation is constructed,

$$\frac{\partial \eta_q}{\partial t} = -M\left(\varphi_q\right)\frac{\delta F}{\delta \eta_q}, q = 1-3 \tag{10}$$
$$\frac{\partial c}{\partial t} = \nabla\cdot\left(\frac{D(T)}{f_{cc}}\nabla(f_c)\right) \tag{11}$$

The total energy F can be expressed as follows, where the first integral term denotes the free energy, including the contribution of the chemical free energy and the gradient energy. The second term E^{ela} denotes the elastic strain energy.

$$F\left(c,\{\eta_q\},T\right) = \int_v\left[f\left(c,\{\eta_q\},T\right) + \sum_{q=1}^{3}\frac{\varepsilon^2(\varphi_q)}{2}\left(\nabla\eta_q\right)^2\right]dv + E^{ela} \tag{12}$$

In the simulation, the precipitate variants in the direction of 0, 60 and 120 degrees are referred to as variant-1, variant-2 and variant-3, respectively. The eigenstrain tensor of precipitation transformation of variant-q, and its matrix form for variant-1 is denoted by $\varepsilon_{ij}^0(1)$.The eigenstrain tensor of the other two variants can be obtained via coordinate rotation transformation as follows [25],

$$\varepsilon_{ij}^0(2) = (R\ \ 60°)\varepsilon_{ij}^0(1)(R\ \ 60°) \tag{13}$$
$$\varepsilon_{ij}^0(3) = (R\ \ 120°)\varepsilon_{ij}^0(1)(R\ \ 120°) \tag{14}$$

where $(R\ \ 60°)$ and $(R\ \ 120°)$ are rotation transformation matrices, and $(R\ \ 60°)$ can be obtained as follows,

$$(R\ \ 60°) = \begin{pmatrix} cos60° & sin60° & 0 \\ -sin60° & cos60° & 0 \\ 0 & 0 & 1 \end{pmatrix} \tag{15}$$

Mesh induced anisotropy is a common issue in phase field simulation and it is more serious when interfacial anisotropy has to be dealt with in a simulation [26]. In order to reduce the mesh induced anisotropy, a special numerical technique based on two sets of mesh, a hexagonal and an orthogonal, was employed to simulate the multi-variant precipitation. The hexagonal mesh was used to solve the phase field governing equations, and the orthogonal mesh was adopted to compute the elastic strain energy. The numerical technique based on the two sets of mesh combines the advantages of the hexagonal mesh in dealing with the precipitate orientation and those of the orthogonal mesh in computing the elastic strain energy. Fig. 1(a) shows the layout of the two meshes in two dimensions, where the hexagonal mesh is in red and the orthogonal in blue, and the two sets of mesh were coupled via data interpolation. Fig. 1(b) shows the layout of the hexagonal mesh and orthogonal mesh in three dimensions.

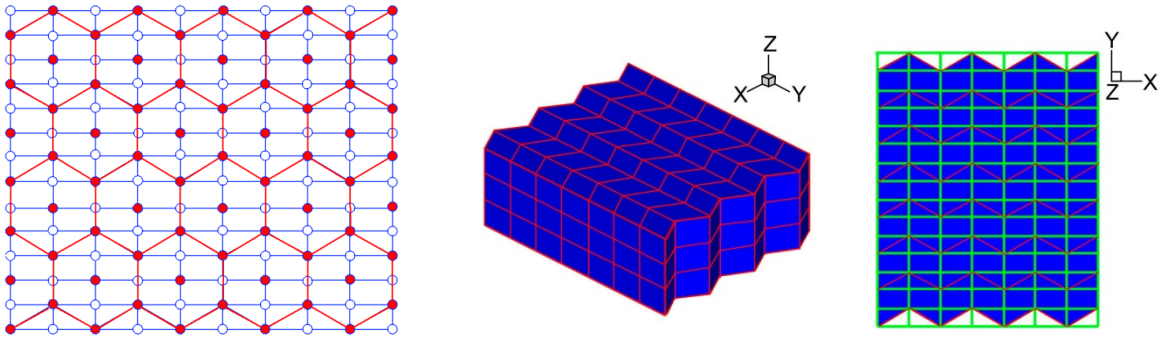

Figure 1. A schematic of the hexagonal and orthogonal mesh employed in simulation, (a) 2D, and (b) 3D

3. Results and discussion

3.1. Pressurized solidification

According to the above calculation method of Gibbs free energy under pressure, the Gibbs free energy of Mg-Al alloy increases with the increase of pressure, which also increases the thermodynamic driving force of the system and expedites the dendritic growth. However the pressure inhibits the solute diffusion as shown in equation (9), which impedes the dendritic growth. The overall effect of pressure on dendritic growth of Mg-9 wt.%Al alloy is shown by the phase field simulation results in Fig. 2, where Δt is the simulation time step, and Fig. 3 shows the solute concentration profile. The simulation is carried out under isothermal condition with the temperature of 851K.

It can be seen from Fig. 2 that the dendritic growth rate under 100MPa tends to increase compared with that under atmospheric pressure and the second dendrite arms are more developed. The solute concentration profile of Fig. 3 shows that due to the fast dendritic growth rate and the decreased solute diffusion coefficient, the solute rejected from the transformation from liquid to solid phase accumulates at the roots of the dendrite arms, which enhances the branch of microstructure.

From the comparison of the morphology of the typical dendrites under atmospheric and 100MPa pressure shown in Fig. 4, the primary dendrite arms under atmospheric pressure are bolder than that under elevated pressure. While with the pressure applied, the primary dendrite arms become slimmer and the secondary dendrite arms are more developed. The simulation results agree well with the experiment results comparing Fig. 2 with Fig. 4.

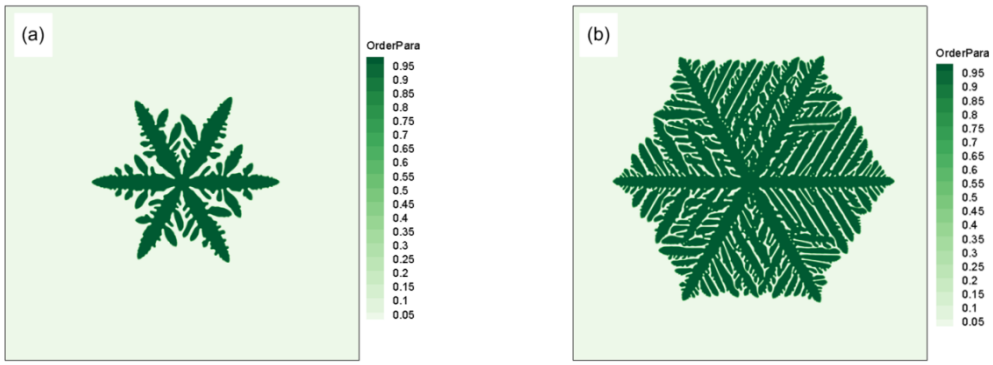

Figure 2. Phase field profile for isothermal solidification simulation at temperature T=851K of dendritic growth of Mg-9 wt.%Al alloy at t=10000Δt, (a) under atmospheric pressure, and (b) under 100MPa

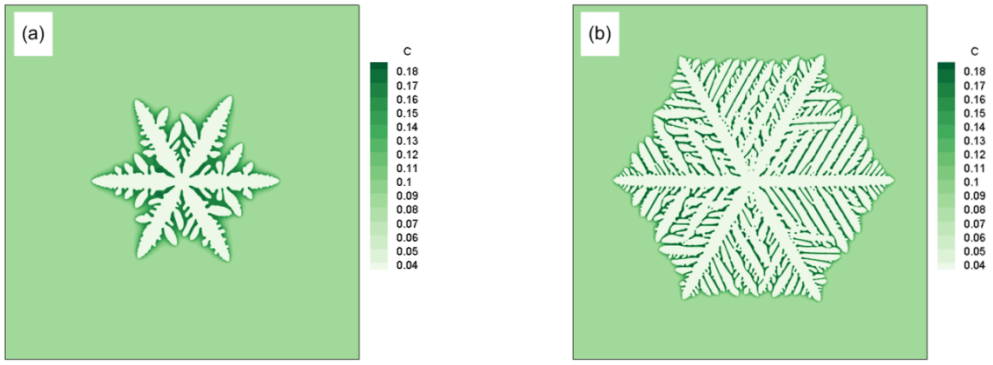

Figure 3. Solute concentration profile for isothermal solidification simulation at temperature T=851K of the dendritic growth of Mg-9 wt.%Al alloy at t=10000Δt, (a) under atmospheric pressure, and (b) under 100MPa

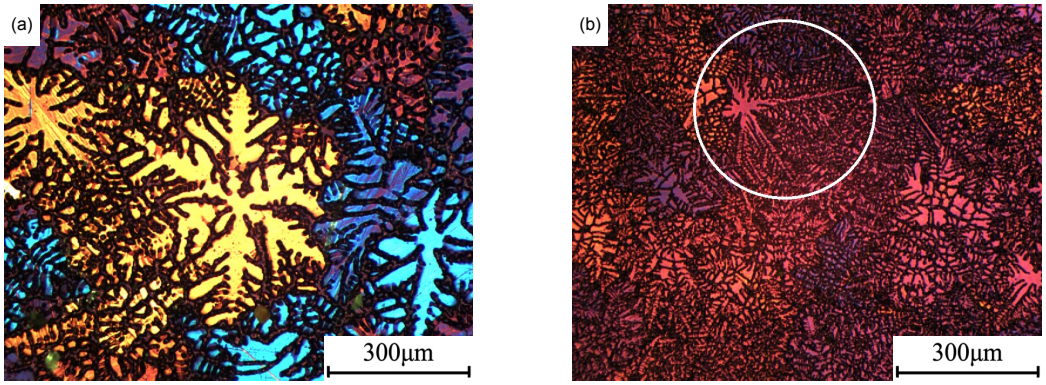

Figure 4. Typical dendrites of AZ91D Mg-Al alloy, (a) under atmospheric pressure, and (b) under 100MPa

3.2. Precipitation process

Fig. 5(a) shows 2D simulation results of the multi-variant precipitates at 1600 seconds, where both the interface anisotropy and the elastic strain energy were taken into account. The blue areas in Fig. 5(a) are the matrix, and the red areas represent the precipitate phase. It can be seen that the precipitate

phase has a lath shape with lozenge ends, and the three variants distribute in the directions with an interval of 60 degrees. Fig. 5(b) is the TEM bright-field image obtained from AZ91 aged at 441K for 16 hours, where three typical precipitate variants with lath shape and lozenge ends can be seen in the basal plane. The angle between the variant-1 and variant-2 is about 80 degrees, and the angle between variant-1 and variant-3 is about 120 degrees. The simulation results of the morphology and distribution of the precipitate variants show a good agreement with the experimental observations.

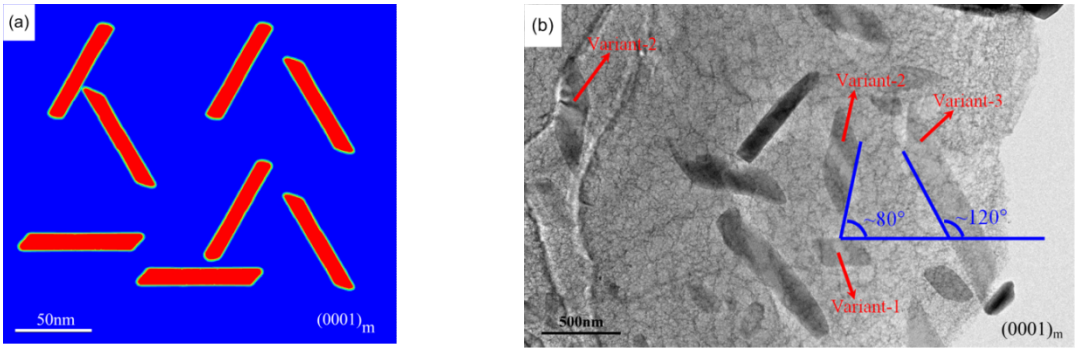

Figure 5. The simulation and TEM observation of multi-variant precipitation, (a)simulation results, and (b) TEM bright-field image of the precipitates for AZ91 aged at 441k for 16 hours

3D simulation on the morphology and distribution of the precipitate variants was carried out as well. In the simulation, a 256 × 256 × 256 hexagonal mesh was employed to solve the phase-field equations, and a 256 × 512 × 256 orthogonal mesh was adopted to calculate the elastic strain energy, which represents a real domain of about 2.22μm × 2.56μm × 2.08μm. The simulation domain is large enough that it is feasible to explore the peak-hardening stage of precipitation during the aging process of this alloy and to predict its properties. In the simulation, the initial compositions of the precipitates and the matrix are 0.4 (molar fraction) and 0.076, respectively. The temperature of the domain was set to 573.15K. To reduce the computation time, parallel computing was employed. The entire parallel numerical calculation was executed on the high-performance cluster computing platform of the Tsinghua National Laboratory for Information Science and Technology.

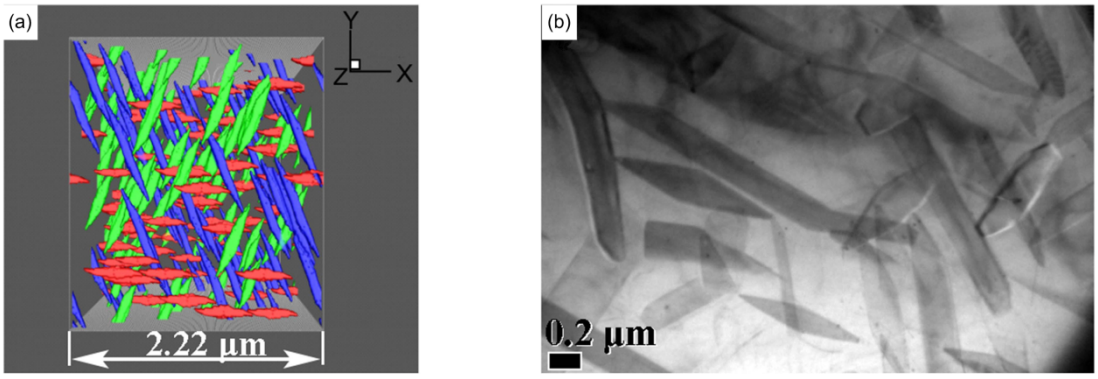

Figure 6. Simulations and TEM observations of multi-variant precipitation in AZ91 aged at 573.15K for 2 hours, (a) simulation results in the xy plane, i.e., (0001) plane of the matrix, t = 2 hours, and (b) TEM image of the precipitates in the basal plane

Fig. 6 shows the 3D simulation results and experimental results for the multi-variant precipitates. In the simulation, the xy plane denotes the (0001) plane of the matrix, and the red, blue, and green laths in Fig. 6(a) are the variant-1, variant-2, and variant-3 precipitates, respectively. It can be seen that

many long lath-shaped precipitates with lozenge ends appear in the simulation domain, and the three variants are oriented in different directions with intervals of about 60 degrees. Fig. 6(b) shows TEM images of multi-variant precipitates viewed in the basal plane, for AZ91 alloy aged at 573.15K for 2 hours. The simulation results are in good agreement with the experimental observations in terms of the variant morphology and distribution.

4. Conclusions

A phase field model coupled with thermodynamic calculation for describing the dendritic growth in pressurized solidification of Mg-Al alloy during squeeze casting has been developed, in which the effects of the pressure on the Gibbs free energy and chemical potential of solid and liquid phases, the solute diffusion coefficient were considered.

2D and 3D phase-field models have been developed to simulate the multi-variant β-$Mg_{17}Al_{12}$ phase precipitation in the aging process of Mg-Al alloy, considering the effects of elastic strain energy, anisotropy of interfacial energy, and anisotropy of interface mobility coefficient.

For pressurized solidification, the dendritic growth rate tends to increase and the secondary dendrite arms are more developed as the pressure is increased from 0.1 to 100MPa, which showed a good agreement with the experimental results of direct squeeze casting of Mg-Al alloy.

For precipitation process, multi-variant precipitates were simulated in 2D and 3D. The simulated precipitates had lath shapes with lozenge ends, and the precipitate variants were parallel to the basal plane and oriented in directions with an angular interval of 60 degrees, which is in good agreement with experimental observations.

Acknowledgements

This work is funded by the National Natural Science Foundation of China (Grant No. 51175291), Tsinghua University Initiative Scientific Research Program (Grant No. 2011Z02160), and the State Key Laboratory of Materials Processing and Die & Mold Technology, Huazhong University of Science and Technology. The support of the State Key Laboratory of Automotive Safety and Energy, Tsinghua University under the contract 2013XC-A-01 is also gratefully acknowledged.

References

[1] Mordike B L and Ebert T 2001 *Mater. Sci. Eng.* A **302** 37
[2] Ghomashchi M R and Vikhrov A 2000 *J. Mater. Process. Technol.* **101** 1
[3] Celotto S 2000 *Acta Mater.* **48** 1775
[4] Yu X F, Zhang G Z, Wang X Y, Gao Y Y, Jia G L and Hao Z Y 1999 *J. Mater. Sci.* **34** 4149
[5] Zhao S S, Peng Q M, Li H and Liu B Z 2014 *J. Alloys Compd.* **584** 56
[6] Kagaya H M, Suzuki T, Takaya M S and Soma T 2001 *Physica* B **293** 343
[7] Sun Z Z, Hu H and Niu X P 2011 *J. Mater. Process. Technol.* **211** 1432
[8] Amin K M and Mufti N A 2012 *J. Mater. Process. Technol.* **212** 1631
[9] Yong M S and Clegg A J 2004 *J. Mater. Process. Technol.* **145** 134
[10] Abou El-khair M T 2005 *Mater. Lett.* **59** 894
[11] Nie J F 2004 *Acta Mater.* **52** 795
[12] Nie J F 2006 *Metall. Mater. Trans.* A **37** 841
[13] Hutchinson C R, Nie J F and Gorsse S 2005 *Metall. Mater. Trans.* A **36** 2093
[14] Böttger B, Eiken J, Ohno M, Klaus G, Fehlbier M, Schmid-Fetzer R, Steinbach I and Bührig-Polaczek A 2006 *Adv. Eng. Mater.* **8** 241
[15] Böttger B, Eiken J and Steinbach I 2006 *Acta Mater.* **54** 2697
[16] Börzsönyi T, Tóth-Katona T, Buka A and Gránásy L 1999 *Phys. Rev. Lett.* **83** 2853
[17] Börzsönyi T, Tóth-Katona T, Buka A and Gránásy L 2000 *Phys. Rev.* E **62** 7817
[18] Li M, Zhang R J and Allison J 2010 *Magnesium Technology* 623
[19] Gao Y P, Liu H, Shi R, Zhou N, Xu Z, Zhu Y M, Nie J F and Wang Y Z 2012 *Acta Mater.* **60** 4819

[20] Han G M, Han Z Q, Luo A A, Sachdev A K and Liu B C 2012 *IOP Conf. Series: Mater. Sci. Eng.* **33** 012110
[21] Kim S G, Kim W T and Suzuki T 1999 *Phys. Rev.* E **60** 7186
[22] Lukas H, Fries S G and Sundman B 2007 *Computational Thermodynamics: The Calphad Method* (London: Cambridge University Press)
[23] Brosh E, Makov G and Shneck R Z 2007 *Calphad* **31** 173
[24] Xu R 2005 *Mater. Lett.* **59** 2818
[25] Han G M, Han Z Q, Luo A A, Sachdev A K and Liu B C 2013 *Scripta Mater.* **68** 691
[26] Mullis A M 2006 *Comput. Mater. Sci.* **36** 345